

## A method for solving the Schrodinger equation

This article has been downloaded from IOPscience. Please scroll down to see the full text article.

1992 J. Phys. A: Math. Gen. 25 3649

(<http://iopscience.iop.org/0305-4470/25/12/024>)

View [the table of contents for this issue](#), or go to the [journal homepage](#) for more

Download details:

IP Address: 171.66.16.58

The article was downloaded on 01/06/2010 at 16:41

Please note that [terms and conditions apply](#).

## A method for solving the Schrödinger equation

Nathan Poliatzky

Department of Nuclear Physics, The Weizmann Institute of Science, Rehovot, Israel

Received 25 October 1991

**Abstract.** We discuss a method for solving the Schrödinger equation with spherically symmetric potentials. The method is based on the use of a certain integral transform for the radial wavefunction. In the representation defined by this transform the Schrödinger equation becomes an integral equation of Volterra type. In a number of cases this equation can be solved exactly without any use of perturbation theory. The resulting solution is represented by a locally finite sum of functions, which can be easily calculated since they are defined by integrals involving simple algebraic functions. For this reason, the method is well suited for practical calculations. In the present article we derive exact solutions for the Yukawa and exponential potentials. As an application we calculate the bound state spectrum and the scattering cross-sections.

### 1. Introduction

In this paper we address the problem of constructing exact solutions for the single-particle Schrödinger equation with a spherically symmetrical potential. We introduce a method based on a new integral transform and discuss its application to two problems: the Yukawa and exponential potentials. The essence of the method is a transformation of the radial Schrödinger equation into an integral equation which is much easier to solve than the original equation. The solutions are given in terms of a locally finite sum of functions which can be easily calculated.

Consider the radial Schrödinger equation for a stationary state of energy  $E = k^2/2m$

$$\left( -\frac{d^2}{dr^2} - \frac{2}{r} \frac{d}{dr} + \frac{l(l+1)}{r^2} + V(r) - k^2 \right) \psi(r) = 0 \quad (1)$$

where  $V(r) = 2mU(r)$ ,  $U(r)$  is an interaction potential,  $m$  is the mass of the particle or a reduced mass of a two-particle system and  $l = 0, 1, \dots$  are the angular momentum quantum numbers. We consider  $k$  to be either real or pure imaginary in which case the energy becomes negative and we are dealing with bound states. If the potential at the origin is less singular than  $r^{-2}$ , equation (1) implies that either  $\psi(r) \propto r^l$  or  $\psi(r) \propto 1/r^{l+1}$  at the origin. For obvious reasons we are primarily interested in the first type of solution. Hence, the correct boundary condition for the above equation is

$$\lim_{r \rightarrow 0} \psi(r) \propto r^l. \quad (2)$$

However, it turns out to be quite useful to construct two independent solutions  $\psi^+(k, r)$  and  $\psi^-(k, r)$ , such that  $\psi^\pm(k, r) \propto 1/r^{l+1}$  at the origin. Since they are independent the desired regular solution can be obtained as their linear superposition

$$\psi(r) = A_l(k)(\psi^-(k, r) - S_l(k)\psi^+(k, r)). \quad (3)$$

Here the constant  $A_l(k)$  controls the normalization of the wavefunction, whereas  $S_l(k)$  controls the behaviour at the origin and can be determined by (2). We now specify the wavefunctions  $\psi^-(k, r)$  and  $\psi^+(k, r)$  by making the ansatz

$$\psi^\mp(k, r) = r^l e^{\mp ikr} \int_0^\infty d\mu e^{-\mu r} \mu^l (\mu \pm 2ik)^l \rho_{\pm k}(\mu). \quad (4)$$

It will be shown below that:

(i) The above ansatz and the fact that  $\psi^\mp(k, r)$  are solutions of (1), lead to the equation for  $\rho_k(\mu)$

$$\rho_k(\mu) = 1 + \int_0^\mu \frac{d\mu'}{[\mu'(\mu' + 2ik)]^{l+1}} \frac{\partial}{\partial \mu'} \int_0^{\mu'} d\mu'' \mathcal{V}(\mu' - \mu'') [\mu''(\mu'' + 2ik)]^l \rho_k(\mu'') \quad (5)$$

where  $\mathcal{V}(\mu)$  is the inverse Laplace transform of the potential, and to a similar equation for  $\rho_{-k}(\mu)$ , which can be obtained by changing  $k$  to  $-k$  in (5). The above equation is a regular Volterra equation of the second kind, provided that the potential vanishes at infinity faster than  $r^{-1}$ .

(ii) The relation between the  $S$ -matrix and a solution of (5) is

$$S_l(k) = \frac{\rho_k(\infty)}{\rho_k^*(\infty)}. \quad (6)$$

(iii) The condition which selects bound states from other solutions of (5) is

$$\rho_{-i\gamma}(\infty) = 0 \quad (7)$$

where  $\gamma \geq 0$ .

The method thus amounts to a change of representation from the configuration representation defined by (1), to the representation where the radial Schrödinger equation is replaced by the integral equation (5). The transformation between the two representations is determined by equations (3) and (4). The method is most effective for potentials containing an exponential factor at large distances. The reason for that is illustrated by the Yukawa potential  $V(r) = -\eta e^{-\mu_0 r}/r$ , for which  $\mathcal{V}(\mu) = -\eta\theta(\mu - \mu_0)$  and (5) becomes

$$\rho_k(\mu) = 1 - \eta\theta(\mu - \mu_0) \int_{\mu_0}^\mu d\mu' \frac{[(\mu' - \mu_0)(\mu' - \mu_0 + 2ik)]^l}{[\mu'(\mu' + 2ik)]^{l+1}} \rho_k(\mu' - \mu_0). \quad (8)$$

Because of the delay in the argument of  $\rho_k(\mu' - \mu_0)$ , this equation is easily solved by a finite number of iterations for each fixed  $\mu$ . With this solution, the binding energies are calculated by replacing (7) by  $\rho_{-i\gamma}(\mu) = 0$  and increasing  $\mu$  until  $\gamma$  does not change within some accuracy limit. The  $S$ -matrix (6) is calculated in a similar way.

A similar method was introduced by Martin for the investigation of analytic properties of the partial wave scattering amplitudes [1, 2]. For the case of an  $S$ -wave ( $l=0$ ) the integral equation which he derived is similar to (5). In fact, if one substitutes  $\rho_k(\mu) = 1 + \int_0^\mu d\mu' \hat{\rho}_k(\mu')$  into (5) and differentiates once with respect to  $\mu$ , one obtains Martin's equation. However, in the case of higher angular momenta, there is no immediate relation between Martin's equation (equation (2.9) in [2]) and equation (5) since the former contains Legendre functions of both types in the integrand, whereas the latter only simple algebraic functions. The appearance of Legendre functions in the kernel of Martin's equation makes it unsuited to the solution of problems such as the calculation of the bound state spectrum or of scattering cross-sections. Equation

(5), on the other hand, is a relatively simple integral equation and is an efficient tool for practical calculations in a number of cases. This will be illustrated below, where we derive exact solutions of (5) for the Yukawa and exponential potentials. These solutions are given in terms of a locally finite sum of functions which can be easily calculated for any given value of the argument. As an application we calculate the bound state spectrum and the scattering cross-sections.

## 2. Integral representation of the radial Schrödinger equation

We derive equation (5) in two steps. First we introduce a pair of auxiliary functions  $\chi^\mp(k, r)$

$$\psi^\mp(k, r) = r^l e^{\mp ikr} \chi^\mp(k, r). \quad (9)$$

From the radial Schrödinger equation and equation (3) we obtain

$$\left( \frac{d^2}{dr^2} + \left( \frac{2(l+1)}{r} - 2ik \right) \frac{d}{dr} - 2ik \frac{l+1}{r} - V(r) \right) \chi^-(r) = 0 \quad (10)$$

and a similar equation for  $\chi^+(r)$ , which can be obtained by changing  $k$  to  $-k$  in (10). The next step is to introduce the integral transform

$$\chi^\mp(k, r) = \int_0^\infty d\mu e^{-\mu r} \mu^l (\mu \pm 2ik)^l \rho_{\pm k}(\mu) \quad (11)$$

and another one for the potential

$$V(r) = \int_0^\infty d\mu e^{-\mu r} \mathcal{V}(\mu). \quad (12)$$

Both integral transforms are invertible. After integration by parts and a change of variable, equation (10) becomes

$$\begin{aligned} & [\mu(\mu + 2ik)]^{l+1} \rho_k(\mu) - 2(l+1) \int_0^\mu d\mu' (\mu + ik) [\mu'(\mu' + 2ik)]^l \rho_k(\mu') \\ &= \int_0^\mu d\mu' \mathcal{V}(\mu - \mu') [\mu'(\mu' + 2ik)]^l \rho_k(\mu'). \end{aligned} \quad (13)$$

Differentiating both sides, then dividing by  $[\mu(\mu + 2ik)]^{l+1}$  and finally integrating the resulting equation, one obtains

$$\begin{aligned} \rho_k(\mu) &= \rho_k(0) + \int_0^\mu \frac{d\mu'}{[\mu'(\mu' + 2ik)]^{l+1}} \frac{\partial}{\partial \mu'} \\ &\quad \times \int_0^{\mu'} d\mu'' \mathcal{V}(\mu' - \mu'') [\mu''(\mu'' + 2ik)]^l \rho_k(\mu''). \end{aligned} \quad (14)$$

Since we are dealing with a second-order equation, there are only two independent integration constants which are  $A_l(k)$  and  $S_l(k)$ . Therefore  $\rho_k(0)$  can be chosen arbitrarily (except for  $\rho_k(0) = 0$  since (14) then has no solutions) and

$$\rho_k(0) = 1 \quad (15)$$

is the most convenient choice. This establishes (5). Despite its uncommon form, it is a conventional inhomogeneous Volterra equation of the second kind. This is seen explicitly if we integrate by parts with respect to  $\mu'$  to obtain

$$\rho_k(\mu) = 1 + \int_0^\mu d\mu' K_k(\mu, \mu') \rho_k(\mu') \tag{16}$$

where the kernel  $K_k(\mu, \mu')$  is given by

$$K_k(\mu, \mu') = [\mu'(\mu' + 2ik)]^l \frac{\partial}{\partial \mu'} \int_\mu^{\mu'} d\mu'' \frac{\mathcal{V}(\mu'' - \mu')}{[\mu''(\mu'' + 2ik)]^{l+1}}. \tag{17}$$

Obviously, since the denominator in (5) becomes zero at  $\mu' = 0$ , the equation does not automatically represent a regular integral equation. Rather, the potential must satisfy a condition to ensure that no singularities appear. To obtain this condition we denote the inverse Laplace transform of the potential in the vicinity of  $\mu = 0$  by  $\mathcal{V}(\mu) = \mathcal{V}_0 + \mathcal{V}_1(\mu)$ , where the second term is assumed to vanish at  $\mu = 0$ . Substituting in (5), one deduces that it is the first term which leads to an infinite contribution, whereas that of the second term is finite. Therefore, a necessary and sufficient condition for the absence of singularities in (5) is

$$\mathcal{V}(0) = 0. \tag{18}$$

To see what this condition amounts to in the configuration space representation, we integrate (12) by parts and take the limit  $r \rightarrow \infty$ . We obtain

$$0 = \lim_{r \rightarrow \infty} \int_0^\infty d\mu \mathcal{V}'(\mu) e^{-\mu r} = \lim_{r \rightarrow \infty} rV(r) - \mathcal{V}(0) \tag{19}$$

and therefore

$$\mathcal{V}(0) = 0 \Leftrightarrow \lim_{r \rightarrow \infty} rV(r) = 0. \tag{20}$$

Thus, for the integral equation (5) to be non-singular, it is necessary and sufficient that the potential vanishes at infinity faster than  $r^{-1}$ . Consequently, equation (5) is non-singular for the Yukawa potential, whereas for the coulomb potential it is singular. Thus, the transition in which the mass of the exchanged particle is taken to zero is a possible way to deal with the singular case.

A few observations now follow on the basis of the above integral representation defined jointly by (9) and (11), i.e. by

$$\psi^\mp(k, r) = r^l e^{\mp ikr} \int_0^\infty d\mu e^{-\mu r} \mu^l (\mu \pm 2ik)^l \rho_{\pm k}(\mu). \tag{4}$$

Since the potential  $\mathcal{V}(\mu)$  is real, (5) implies

$$\rho_k^*(\mu) = \rho_{-k}(\mu). \tag{21}$$

From this and (4) we have

$$(\psi^\mp(k, r))^* = \psi^\pm(k, r). \tag{22}$$

Hence from (3) and from the fact that  $\psi(r)$  is real, it follows that

$$S_l^*(k) = \frac{1}{S_l(k)}. \tag{23}$$

Hence we can write

$$S_l(k) = e^{2i\delta_l(k)}. \quad (24)$$

This suggests that  $S_l(k)$  is identical with the  $S$ -matrix and indeed one can verify that this is the case.

For the interaction-free case,  $\mathcal{V}(\mu) = 0$ , equation (5) implies  $\rho_k(\mu) = 1$ . Substituting this into (4) we obtain

$$\psi^+(k, r) = r^l e^{ikr} \int_0^\infty d\mu e^{-\mu r} \mu^l (\mu - 2ik)^l \equiv i l! (2k)^l \sqrt{\frac{\pi k}{2r}} H_{l+1/2}^{(1)}(kr) \quad (25)$$

and

$$\psi^-(k, r) = r^l e^{-ikr} \int_0^\infty d\mu e^{-\mu r} \mu^l (\mu + 2ik)^l \equiv -i l! (2k)^l \sqrt{\frac{\pi k}{2r}} H_{l+1/2}^{(2)}(kr) \quad (26)$$

where  $H_{l+1/2}^{(1)}$  and  $H_{l+1/2}^{(2)}$  are Hankel functions. From (3) and  $2J_{l+1/2} \approx H_{l+1/2}^{(1)} + H_{l+1/2}^{(2)}$  it follows that

$$\psi(r) = -i A_l(k) l! (2k)^l \sqrt{\frac{\pi k}{2r}} (2J_{l+1/2}(kr) + (S_l(k) - 1) H_{l+1/2}^{(1)}(kr)) \quad (27)$$

where  $J_{l+1/2}$  is the Bessel function. Near the origin this Bessel function behaves as  $r^{l+1/2}$ , whereas the Hankel function behaves as  $1/r^{l+1/2}$ . Therefore, in order for the wavefunction  $\psi(r)$  to behave near the origin as specified in (2), the second term in the above equation must vanish and we have

$$S_l(k) = 1 \quad (28)$$

and

$$\psi(r) = -i A_l(k) l! (2k)^{l+1/2} \sqrt{\frac{\pi}{r}} J_{l+1/2}(kr). \quad (29)$$

If the interaction is present one cannot, of course, deduce the explicit form of the  $S$ -matrix  $S_l(k)$ , but one can determine its relation to  $\rho_k$ . To do this we insert (4) into (3) and let  $r \rightarrow 0$ . In this limit the asymptotically large values of  $\mu$  are dominant, hence we have

$$\lim_{r \rightarrow 0} \psi(r) = \frac{A_l(k) (2l)!}{r^{l+1}} (\rho_k(\infty) - S_l(k) \rho_{-k}(\infty)) + O\left(\frac{1}{r^l}\right). \quad (30)$$

Therefore, a necessary condition for  $\lim_{r \rightarrow 0} \psi(r) \propto r^l$  is

$$S_l(k) = \frac{\rho_k(\infty)}{\rho_{-k}(\infty)}. \quad (31)$$

Now it is well known that if the potential is less singular than  $r^{-2}$  at the origin, all solutions of the radial Schrödinger equation behave either like  $\psi(r) \propto r^l$  or  $\psi(r) \propto 1/r^{l+1}$  at the origin. Therefore, if in a superposition of two solutions of the second type, the coefficients are chosen in such a way as to make the lowest power of  $r$  vanish, the resulting solution will automatically be of the first type. This means that (31) is not only a necessary but also a sufficient condition. Using (21), we can write this condition in a more convenient form

$$S_l(k) = \frac{\rho_k(\infty)}{\rho_k^*(\infty)}. \quad (32)$$

In the case of bound states the energy is negative,  $E = k^2/2 \leq 0$ , and consequently momentum is purely imaginary,  $k = \pm i\gamma$ . Consider the case  $k = i\gamma$ , where  $\gamma > 0$ . The wavefunction  $\psi(i\gamma, r)$  grows exponentially at infinity, which is unacceptable. Consequently, we must put  $A_l(i\gamma) = 0$  and  $A_l(i\gamma)S_l(i\gamma) = -a_l(\gamma)$ , where  $a_l(\gamma)$  is finite. From (3) we then have

$$\psi(r) = a_l(\gamma)r^l e^{-\gamma r} \int_0^\infty d\mu e^{-\mu r} \mu^l (\mu + 2\gamma)^l \rho_{-i\gamma}(\mu) \quad (33)$$

which is the wavefunction of a bound state. If  $\rho_{-i\gamma}(\mu)$  is not oscillating as  $\mu \rightarrow \infty$  and  $\rho_{-i\gamma}(\infty)$  is non-zero then as  $r \rightarrow 0$  the above integral behaves as  $1/r^{l+1}$ . Therefore, a necessary condition for  $\lim_{r \rightarrow 0} \psi(r) \propto r^l$  is

$$\rho_{-i\gamma}(\infty) = 0 \quad (34)$$

or else  $\rho_{-i\gamma}(\mu)$  must oscillate as  $\mu \rightarrow \infty$ . The same argument as the one given after (31) proves that this condition is also sufficient. This condition selects discrete bound state energies; without it (5) can be solved for any value of the energy. The case of oscillating  $\rho_{-i\gamma}(\mu)$  is considered in detail in [3]. Here we will not be concerned with this case and hence will be concerned with (34) only. Notice that for the  $S$ -matrix we have

$$S_l(i\gamma) = \infty \quad (35)$$

i.e. bound states appear as singularities of the  $S$ -matrix. Alternatively we could consider the case  $k = -i\gamma$ , where  $\gamma \geq 0$ . We obtain the same equations (33) and (34) with  $a_l(\gamma)$  replaced by  $A_l(-i\gamma)$ . The only difference is that now

$$S_l(-i\gamma) = 0. \quad (36)$$

Thus, we notice that in the present context, bound states correspond to singularities and zeros of the  $S$ -matrix.

### 3. Yukawa potential

The Yukawa potential

$$U(r) = -\frac{f^2}{4\pi} \frac{e^{-\mu_0 r}}{r} \quad (37)$$

was originally introduced into nuclear physics by Yukawa [4]. At that time it was thought that the Yukawa potential, which describes the interaction between nucleons as mediated by a pion exchange, represents the strong force in nuclei. Today we know that only the long-range part of the nucleon-nucleon interaction is dominated by a pion exchange and that, at smaller distances, other particles (most probably spin 1) enter the exchange mechanism and dominate it. Yet, in some sense, Yukawa potential is the most fundamental potential in quantum mechanics since exchange of a particle is the most basic interaction mechanism. There have been many attempts to obtain exact solutions for the Schrödinger equation with the Yukawa potential, but little has been published [5].

The inverse Laplace transform of the potential  $V(r) = 2mU(r)$  is

$$\mathcal{V}(\mu) = -\eta\theta(\mu - \mu_0) \quad (38)$$

where  $\eta = 2mf^2/4\pi$  and  $\theta(\mu - \mu_0)$  is the step function which vanishes for  $\mu < \mu_0$ , equals 1/2 for  $\mu = \mu_0$  and is equal to 1 otherwise. Substituting (38) in (5) we obtain

$$\rho_k(\mu) = 1 - \eta\theta(\mu - \mu_0) \int_{\mu_0}^{\mu} d\mu' \frac{[(\mu' - \mu_0)(\mu' - \mu_0 + 2ik)]^l}{[\mu'(\mu' + 2ik)]^{l+1}} \rho_k(\mu' - \mu_0). \quad (39)$$

If we introduce the dimensionless variables

$$s = \frac{\mu}{\mu_0} \quad \nu = \frac{2ik}{\mu_0} \quad \eta_0 = \frac{\eta}{\mu_0} = \frac{f^2}{4\pi} \frac{2m}{\mu_0} \quad R_\nu(\eta_0, s) = \rho_k(\mu) \quad (40)$$

the above integral equation becomes

$$R_\nu(\eta_0, s) = 1 - \eta_0\theta(s - 1) \int_1^s dt \frac{[(t-1)(t-1+\nu)]^l}{[t(t+\nu)]^{l+1}} R_\nu(\eta_0, t-1). \quad (41)$$

A proper ansatz for the solution of this equation is

$$R_\nu(\eta_0, s) = \sum_{n=0}^{[s]} (-\eta_0)^n \varphi_n(s-n, \nu) \quad (42)$$

where  $[s]$  is the largest integer which is smaller than or equal to  $s$ . Notice that the right-hand side of the above equation is a finite sum. Equation (42) can be identically rewritten as

$$R_\nu(\eta_0, s) = \sum_{n=0}^{\infty} (-\eta_0)^n \theta(s-n) \varphi_n(s-n, \nu). \quad (43)$$

Substituting in (41) and comparing equal powers of  $\eta_0$ , we obtain the recurrence relation for the functions  $\varphi_n$

$$\begin{aligned} \varphi_0(y, \nu) &= 1 \\ \varphi_n(y, \nu) &= \int_0^y dt \frac{[(t+n-1)(t+n-1+\nu)]^l}{[(t+n)(t+n+\nu)]^{l+1}} \varphi_{n-1}(t, \nu) \quad n = 1, 2, \dots \end{aligned} \quad (44)$$

which guarantees that the ansatz is in fact a solution. From this recurrence relation it is clear that the functions  $\varphi_n(y, \nu)$  are analytic functions in the whole complex  $\nu$ -space cut along the negative real axis from  $-\infty$  to  $-1$ . Note that the ansatz (42) has been chosen so that the coupling constant  $\eta_0$  does not appear in the recurrence relation. Therefore, once the  $\varphi_n$  functions are calculated, (41) is solved for any value of the coupling constant. This is an important advantage compared to any numerical solution which can be performed for specified values of the parameters only.

To get some idea of the functions  $\varphi_n$  it is instructive to consider the case of zero energy bound states,  $\nu = 0$ . In this case the first few  $\varphi_n$  functions can be expressed in terms of logarithmic and algebraic functions (see the appendix), while others can be approximated with reasonable accuracy. Such approximations are easily found since the integrand in (44) is a simple algebraic function. For instance,

$$\varphi_n(y, 0) \approx \frac{1}{n!(2l+1)_n} \left(\frac{y}{y+n}\right)^{2l} \frac{y^n}{(y+1)_n} \quad (45)$$

is an approximation which is exact for  $n=0$  and  $n=1$  and approaches the exact  $\varphi_n$  as  $l \rightarrow \infty$ . Here  $(a)_n$  is the Pochhammer symbol defined by  $(a)_n = a(a+1)\dots(a+n-1)$



and  $(a)_0 = 1$ , where  $a = 2l + 1$  and  $a = y + 1$  respectively. Another useful approximation resulting from the recurrence relation (44) is based on

$$\lim_{n \rightarrow \infty} [n! n! \varphi_n(\infty, 0)]^{1/n} = eC \quad l = 0 \tag{46}$$

where  $C = 0.577\ 215\ 66 \dots$  is the Euler-Mascheroni constant. Using (45) or (46) we can estimate the values of the coupling constant at which zero energy bound states appear. From (34), the condition for bound states is

$$R_\nu(\eta_0, \infty) = 0 \tag{47}$$

where  $R_\nu(\eta_0, \infty)$  is given by (42). Using (45) this gives  $J_{2l}(2\sqrt{\eta_0}) = 0$ , and hence for large  $l$  we have  $2\sqrt{\eta_0} = (n_r + l - 1/4)\pi$ , where  $n_r$  should be identified with the radial quantum number. Substituting  $\eta_0 = 2mf^2/4\pi\mu_0$ , we obtain

$$\frac{\pi^2}{4} (n - \frac{1}{4})^2 = \frac{f^2}{4\pi} \frac{2m}{\mu_0} \quad l \gg 0 \tag{48}$$

where  $n = n_r + l$  is the main quantum number. Similarly, from (46) we obtain

$$\frac{\pi^2}{4eC} (n - \frac{1}{4})^2 = \frac{f^2}{4\pi} \frac{2m}{\mu_0} \quad l = 0 \quad n \gg 1. \tag{49}$$

Equations (48) and (49) determine the values of the coupling constant for the zero energy bound states with an accuracy of about 10-20%.

From either (45) or (46) it is clear that the speed of convergence of the series in (47) must be similar to that of a Bessel function, i.e. quite fast. Moreover, it turns out that the speed of convergence increases significantly if we solve

$$R_\nu(\eta_0, n_{\max} + 1) = 0 \tag{50}$$

where  $n_{\max}$  is some integer, instead of truncating the series in (47) at  $n = n_{\max}$ . We consider  $n_{\max} = 3$  as an illustration. Only three functions are then needed:  $\varphi_1(3, 0)$ ,  $\varphi_2(2, 0)$  and  $\varphi_3(1, 0)$ . Inserting the expressions provided in the appendix, we obtain

$$R_0(\eta_0, 4) \equiv 1 - \eta_0^{\frac{3}{4}} + \eta_0^2(\frac{1}{2} - \ln \frac{3}{2}) - \eta_0^3(\frac{1}{4} - \ln \frac{9}{8} - \frac{1}{4} \ln \frac{27}{16}) = 0. \tag{51}$$

Solving this equation for  $\eta_0$  we obtain (the smallest root) the value 1.680 34 for the ground state, which gives the correct result with an accuracy of about 2 parts in  $10^4$ . To achieve this accuracy using (47) would require twice as many terms in  $\eta_0$ .

Since in general one cannot express the functions  $\varphi_n$  in terms of elementary or special functions, one has to devise a numerical algorithm for their evaluation. As a first step we introduce a new variable  $z$

$$z = \frac{y}{1 + \alpha y} \quad y = \frac{z}{1 - \alpha z} \quad 0 < \alpha < \infty \tag{52}$$

where  $\alpha$  is an arbitrary positive number. Notice that the variable  $z$  remains finite even at  $y = \infty$ . To transform the recurrence relations (44) to this variable, we introduce new functions  $\phi_n$

$$\varphi_n(y, \nu) = \frac{\phi_n(z, \nu)}{n!(1 + \nu)_n n^l (n + \nu)^l} \tag{53}$$

The particular form of the denominator in this equation reflects the main dependence of functions  $\phi_n$  on  $n$  for  $y \gg n$ . The recurrence relation now takes the following form:

$$\phi_0(z, \nu) = 1 \quad \phi_n(z, \nu) = \int_0^z dt f_n(t, \nu) \phi_{n-1}(t, \nu) \quad n = 1, 2, \dots \quad (54)$$

where

$$f_1(t, \nu) = \frac{[t(\nu + (1 - \alpha\nu)t)]'}{[(1 + a_1t)(1 + a_{1+\nu}t)]^{l+1}} \quad (55)$$

$$f_n(t, \nu) = \frac{[(1 + a_{n-1}t)(1 + a_{n-1+\nu}t)]^l}{[(1 + a_nt)(1 + a_{n+\nu}t)]^{l+1}} \quad a_\beta = \frac{1}{\beta} - \alpha.$$

As a next step we divide the interval  $[0, z]$  in  $\mathcal{N}$  pieces of length  $x$  and replace the integration in (54) by the summation according to the trapezoidal rule. As the result we obtain the new functions  $\bar{\phi}_n(x_j, \nu)$  which operate on the grid of points  $x_0 \equiv 0, x_1, \dots, x_{\mathcal{N}} \equiv z$  and converge to the true functions  $\phi_n(x_j, \nu)$  in the continuum limit as  $x \rightarrow 0$ . The corresponding recurrence relation is

$$\bar{\phi}_n(x_j, \nu) = x \sum_{i=0}^j \theta(i)\theta(j-i) f_n(x_i, \nu) \bar{\phi}_{n-1}(x_i, \nu) \quad j = 1, \dots, \mathcal{N} \quad (56)$$

where

$$\bar{\phi}_0(x_j, \nu) = 1 \quad \bar{\phi}_n(0, \nu) = 0 \quad n = 1, 2, \dots \quad (57)$$

$x_j = jx$  and where the step function  $\theta$  is defined as above (see (38)). The recurrence process starts with (57) and proceeds to the evaluation of (56) for  $n = 1$  and  $x_j$  iterated from  $x_1$  to  $x_{\mathcal{N}}$ . Then  $n$  is reset to  $n = 2$  and the calculation is repeated. These operations are continued until  $n$  reaches some maximal value  $n_{\max}$ . The result of the whole recurrence process is  $\bar{\phi}_n(x_1, \nu), \dots, \bar{\phi}_n(x_{\mathcal{N}}, \nu), n = 1, \dots, n_{\max}$ . In order to obtain an estimate of the difference between  $\bar{\phi}_n(x_j, \nu)$  and  $\phi_n(x_j, \nu)$ , one refines the grid by replacing  $\mathcal{N}$  by  $2\mathcal{N}$  and  $x$  by  $x/2$  and compares the resulting  $\bar{\phi}_n(x_2, \nu), \dots, \bar{\phi}_n(x_{2\mathcal{N}}, \nu)$  with the previously calculated  $\bar{\phi}_n(x_1, \nu), \dots, \bar{\phi}_n(x_{\mathcal{N}}, \nu)$ . If the difference is below some accuracy limit, then within this accuracy the convergence point can be considered to be reached and  $\bar{\phi}_n(x_1, \nu), \dots, \bar{\phi}_n(x_{2\mathcal{N}}, \nu)$  can be considered to be identical to  $\phi_n(x_1, \nu), \dots, \phi_n(x_{2\mathcal{N}}, \nu)$ . Note that since (56) is an inhomogeneous two-term recurrence relation with respect to  $x_j$ , its solution is unique and there is no danger of instability caused by round-off error.

As an application let us consider the bound state spectrum, i.e. the relation between the coupling constant  $\eta_0 = 2mf^2/4\pi\mu_0$  and the bound state energy  $E$ , or equivalently, between  $\eta_0$  and  $\nu = 2\sqrt{-2mE}/\mu_0$ . Formally this relation is obtained by solving (47). In practice this is done by solving (50) for a large  $n_{\max}$ . Thus

$$\sum_{k=0}^{n_{\max}} (-\eta_0)^k \varphi_k(n_{\max} + 1 - k, \nu) = 0 \quad (58)$$

is the equation determining the bound state spectrum. In table 1 we present the values of the coupling constant  $\eta_0$  at which bound states of zero binding energy appear. Throughout table 1 only accurate digits are shown. No attempt was made to achieve high accuracy. Therefore for a fixed  $n_{\max}$  the accuracy of the values  $\phi_n(z, \nu)$  decreases with increasing  $n$ . The varying accuracy in table 1 reflects the increasing sensitivity of

**Table 1.** Values of the coupling constant  $\eta_0 = 2mf^2/4\pi\mu_0$  at which bound states of zero energy appear in the case of the Yukawa potential.  $l$  and  $n_r$  are the angular and the radial quantum numbers.

| <i>l</i> | <i>n<sub>r</sub></i> |            |            |            |         |         |         |
|----------|----------------------|------------|------------|------------|---------|---------|---------|
|          | 1                    | 2          | 3          | 4          | 5       | 6       | 7       |
| 0        | 1.679 8077           | 6.447 2603 | 14.342 027 | 25.371 659 | 39.5388 | 56.8448 | 77.2904 |
| 1        | 9.081 9589           | 17.744 575 | 29.461 426 | 44.261 253 | 62.1601 | 83.1682 | 107.292 |
| 2        | 21.89 4984           | 34.420 41  | 49.969 57  | 68.5714    | 90.245  | 115.00  | 142.85  |
| 3        | 40.135 55            | 56.5141    | 75.899     | 98.317     | 123.78  | 152.3   | 183     |
| 4        | 63.8089              | 84.036     | 107.2      | 133.5      | 162.7   | 195.1   | 230     |
| 5        | 92.9171              | 116.992    | 144.055    | 174.12     | 207.2   | 243.3   | 282     |
| 6        | 127.460              | 155.382    | 186.28     | 220.1      | 257     | 297     | 340     |

$\eta_0$  on  $\phi_n$  with large  $n$  at high quantum numbers. The data shown in table 1 were obtained with  $n_{\max} = 20$ .

Note that no bound state can exist for  $\eta_0 < 1.67$ , whereas the experimental  $\pi NN$  coupling constant is  $f^2/4\pi \approx 0.08$ , which corresponds to  $\eta_0 \approx 0.57$ . Thus, as is well known, the existence of the deuteron cannot be explained in a non-relativistic model based solely on the pion exchange. The rest of the spectrum is shown in figure 1(a). For the sake of comparison we have included in this figure the four lowest levels for the coulomb potential. Figure 1(b) shows the region of small bound state energies of the spectrum shown in figure 1(a). As one would expect on intuitive grounds, figures 1(a) and (b) show that the spectrum at large binding energies is essentially that of the coulomb potential, whereas at small binding energies the spectrum is dominated by the long-range part of the potential which is completely unlike the coulomb potential. Thus, at large binding energies there is an almost perfect degeneracy in  $l$ , whereas at small binding energies this degeneracy disappears completely. It is interesting to note that the degeneracy in  $l$  appears at much smaller energies than the energy at which the difference between the coulomb and Yukawa spectra becomes negligible.

As another application of the method we consider the calculation of the scattering cross-sections  $\sigma_l(k)$ . The relation between the  $S$ -matrix  $S_l(k)$  and the cross-section  $\sigma_l(k)$  is

$$\sigma_l(k) = \frac{\pi(2l+1)}{k^2} |S_l(k) - 1|^2. \tag{59}$$

Equation (32), on the other hand, provides a direct relation between the  $S$ -matrix  $S_l(k)$  and  $\rho_k$ . In terms of  $\varphi_n$  functions this relation reads

$$S_l(k) = \frac{R_\nu(\eta_0, \infty)}{R_\nu^*(\eta_0, \infty)} \quad R_\nu(\eta_0, \infty) = \sum_{n=0}^{\infty} (-\eta_0)^n \varphi_n(\infty, \nu) \tag{60}$$

where  $\nu = 2ik/\mu_0$ . As in the case of the bound states, only a finite number  $n = n_{\max}$  of summations has to be taken into account to achieve a given accuracy. Because of the fast convergence of the series in (60),  $n_{\max}$  is relatively small. Thus, the above method of solving (5) provides a simple way to calculate the cross-sections  $\sigma_l(k)$ . In figures 2(a)-(c) we present some typical examples of cross-sections. they are calculated with  $n_{\max}$  ranging from 10 to 25.

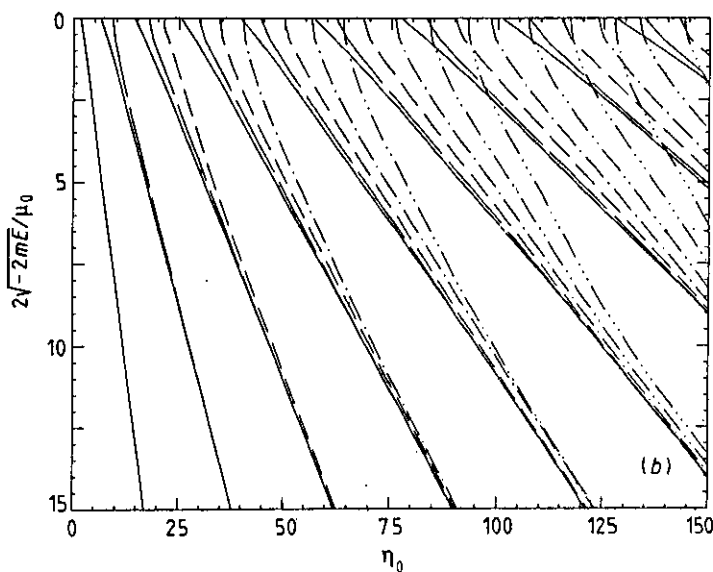
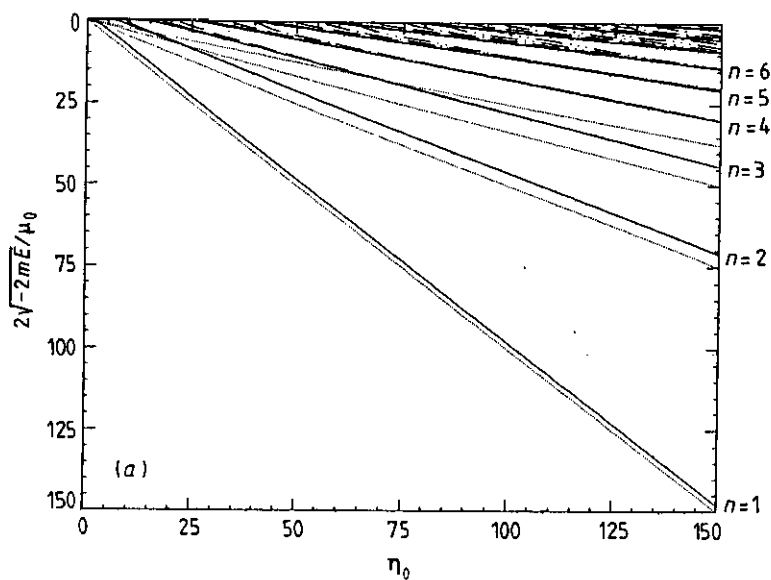


**Figure 1.** (a)  $\nu = 2\sqrt{-2mE}/\mu_0$  as a function of  $\eta_0 = 2mf^2/4\pi\mu_0$  for the Yukawa potential.  $n = n_r + l$  is the main quantum number. Dotted lines represent the four lowest levels for the case of a coulomb potential. (b) The region of small bound state energies of the spectrum shown in (a). The assignment of the angular momentum quantum number  $l$  to different lines is as follows:  $l=0$  (full);  $l=1$  (long dashes);  $l=2$  (medium dashes);  $l=3$  (medium dash and a dot);  $l=4$  (medium dash and two dots);  $l=5$  (medium dash and three dots);  $l=6$  (medium dash and four dots).

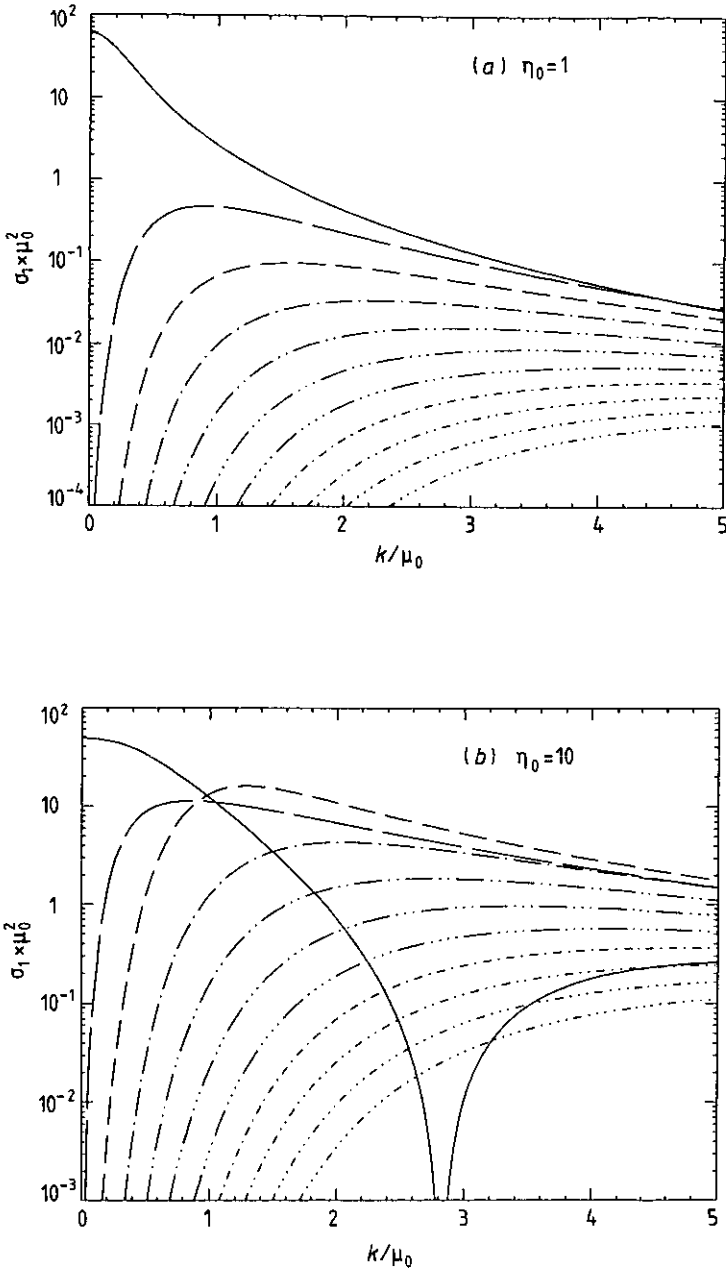


**Figure 2.** (a) Scattering cross-sections for the Yukawa potential for the case of a small coupling constant  $\eta_0 = 2mf^2/4\pi\mu_0 = 1$ . The assignment of the angular momentum quantum number  $l$  to different lines is as follows:  $l=0$  (full);  $l=1$  (long dashes);  $l=2$  (medium dashes);  $l=3$  (medium dash and a dot);  $l=4$  (medium dash and two dots);  $l=5$  (medium dash and three dots);  $l=6$  (medium dash and four dots);  $l=7$  (short dash and a dot);  $l=8$  (short dash and two dots);  $l=9$  (short dash and three dots);  $l=10$  (short dash and four dots). (b) The same as in (a) but for a larger coupling constant  $\eta_0 = 10$ . (c) The same as in (a) but for a still larger coupling constant  $\eta_0 = 30$ .

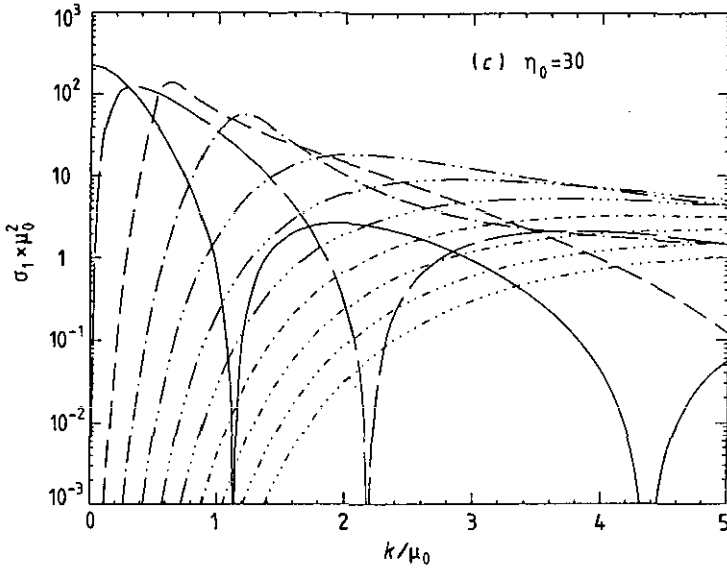


Figure 2. (continued)

#### 4. Exponential potential

The exponential potential

$$U(r) = -U_0 e^{-\mu_0 r} \tag{61}$$

was originally considered by Bethe and Bacher as a model potential for the ground state of the deuteron [6]. The inverse Laplace transform of the potential  $V(r) = 2mU(r)$  is

$$\mathcal{V}(\mu) = -\eta \delta(\mu - \mu_0) \tag{62}$$

where  $\eta = 2mU_0$  and  $\delta$  is the Dirac delta function. Substituting in (5) gives

$$\begin{aligned} \rho_k(\mu) = 1 - \eta \int_0^\mu \frac{d\mu'}{[\mu'(\mu' + 2ik)]^{l+1}} \frac{\partial}{\partial \mu'} \theta(\mu' - \mu_0) \\ \times [(\mu' - \mu_0)(\mu' - \mu_0 + 2ik)]^l \rho_k(\mu' - \mu_0). \end{aligned} \tag{63}$$

As in the case of the Yukawa potential, we now change to dimensionless variables

$$s = \frac{\mu}{\mu_0} \quad \nu = \frac{2ik}{\mu_0} \quad \eta_0 = \frac{\eta}{\mu_0^2} = \frac{U_0}{\mu_0} \frac{2m}{\mu_0} \quad R_\nu(\eta_0, s) = \rho_k(\mu) \tag{64}$$

and obtain

$$R_\nu(\eta_0, s) = 1 - \eta_0 \int_0^s \frac{dt}{[t(t + \nu)]^{l+1}} \frac{\partial}{\partial t} \theta(t - 1) [(t - 1)(t - 1 + \nu)]^l R_\nu(\eta_0, t - 1). \tag{65}$$

Again, as in the case of the Yukawa potential, a proper ansatz proves to be

$$R_\nu(\eta_0, s) = \sum_{n=0}^{[s]} (-\eta_0)^n \varphi_n(s - n, \nu). \tag{66}$$

Substituting in (65) we obtain the following conditions which ensure that the ansatz is in fact a solution

$$\varphi_0(y, \nu) = 1 \quad (67)$$

and

$$\begin{aligned} \varphi_n(y, \nu) = & \frac{[(n-1)(n-1+\nu)]^l}{[n(n+\nu)]^{l+1}} \varphi_{n-1}(0, \nu) \\ & + \int_0^y \frac{dt}{[(t+n)(t+n+\nu)]^{l+1}} \frac{\partial}{\partial t} [(t+n-1)(t+n-1+\nu)]^l \varphi_{n-1}(y, \nu). \end{aligned} \quad (68)$$

Again, the appropriate choice of the ansatz (66) has ensured that the coupling constant  $\eta_0$  does not appear in the recurrence relation. Therefore, once the  $\varphi_n$  functions are calculated the problem is essentially solved for any value of the coupling constant. We emphasize that this is a very important advantage compared to any numerical solution which can be performed for specified values of parameters only.

To proceed further, we first consider the case of zero angular momentum states,  $l=0$ . In this case it is readily seen that all of the  $\varphi_n$  functions are constant in  $y$  and hence the integral in the recurrence relation (68) vanishes identically. The rest of the recurrence relation can be easily iterated resulting in

$$\varphi_n(y, \nu) = \frac{1}{n!(1+\nu)_n} \quad (69)$$

where  $(1+\nu)_n = (1+\nu)(2+\nu) \dots (n+\nu)$  is the Pochhammer symbol ( $(1+\nu)_0 = 1$ ). This leads to the well known (*s*-wave) solution for bound states [6]  $r\psi(r) \propto J_\nu(2\sqrt{\eta_0} e^{-\mu_0 r/2})$ . In the case of non-zero angular momenta  $l \neq 0$ , after integration by parts the recurrence relation (68) becomes

$$\begin{aligned} \varphi_n(y, \nu) = & \frac{[(y+n-1)(y+n-1+\nu)]^l}{[(y+n)(y+n+\nu)]^{l+1}} \varphi_{n-1}(y, \nu) \\ & + 2(l+1) \int_0^y dt \left( t+n+\frac{\nu}{2} \right) \frac{[(t+n-1)(t+n-1+\nu)]^l}{[(t+n)(t+n+\nu)]^{l+2}} \varphi_{n-1}(t, \nu). \end{aligned} \quad (70)$$

As in the case of the Yukawa potential, our aim is to convert the above recurrence relation to an algebraic one and hence we can use the same strategy. We introduce a new variable  $z$

$$z = \frac{y}{1+\alpha y} \quad y = \frac{z}{1-\alpha z} \quad 0 < \alpha < \infty \quad (71)$$

and new functions  $\phi_n$

$$\varphi_n(y, \nu) = \frac{\phi_n(z, \nu)}{n!(1+\nu)_n n^l (n+\nu)^l}. \quad (72)$$

The recurrence relation (70) now takes the following form:

$$\phi_0(z, \nu) = 1 \quad \phi_n(z, \nu) = g_n(z, \nu) \phi_{n-1}(z, \nu) + \int_0^z dt h_n(t, \nu) \phi_{n-1}(t, \nu) \quad n = 1, 2, \dots \quad (73)$$

where

$$g_n(z, \nu) = (1 - \alpha z)^2 f_n(z, \nu) \tag{74}$$

and

$$h_n(t, \nu) = \frac{2(l+1)(n+\nu/2)}{n(n+\nu)} \frac{(1+a_{n+\nu/2}t)(1-\alpha t)}{(1+a_n t)(1+a_{n+\nu}t)} f_n(t, \nu), \quad a_\beta = \frac{1}{\beta} - \alpha. \tag{75}$$

The function  $f_n$  is the same as in (55) and the further procedure is the same as that described after (55), except for the resulting recurrence relation which is now

$$\begin{aligned} \bar{\phi}_n(x_j, \nu) &= g_n(x_j, \nu) \bar{\phi}_{n-1}(x_j, \nu) \\ &+ x \sum_{i=0}^j \theta(i) \theta(j-i) h_n(x_i, \nu) \bar{\phi}_{n-1}(x_i, \nu) \quad j = 1, \dots, \mathcal{N} \end{aligned} \tag{76}$$

where

$$\bar{\phi}_0(x_j, \nu) = 1 \quad \bar{\phi}_n(0, \nu) = 0 \quad n = 1, 2, \dots \tag{77}$$

As an application we consider the bound state spectrum, i.e. the relation between the coupling constant  $\eta_0 = U_0 2m / \mu_0^2$  and  $\nu = 2\sqrt{-2mE} / \mu_0$ . As in the case of the Yukawa potential, this relation is obtained by solving (58). The values of the coupling constant  $\eta_0$  for zero energy bound states are presented in table 2. The remarks made after (58) also apply to table 2. The data shown in table 2 were obtained with  $n_{\max} = 20$ .

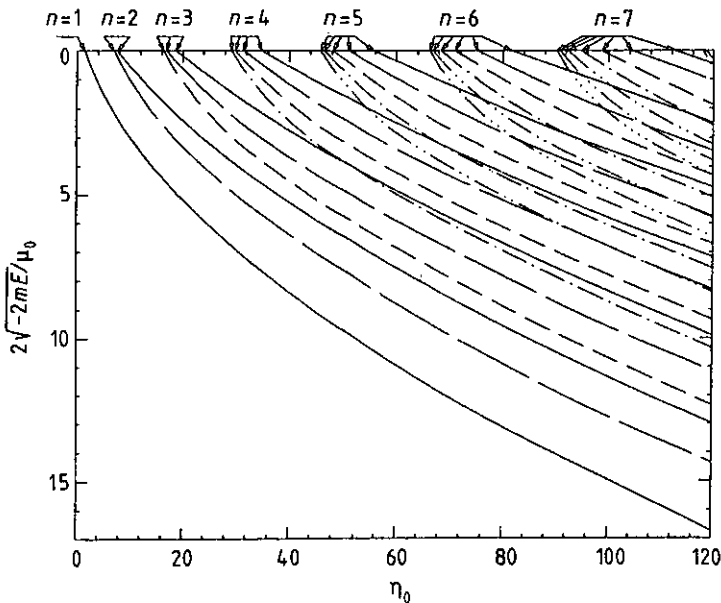


Figure 3.  $\nu = 2\sqrt{-2mE} / \mu_0$  as a function of  $\eta_0 = U_0 2m / \mu_0^2$  for the exponential potential.  $n = n_r + l$  is the main quantum number. The assignment of the angular momentum quantum number  $l$  to different lines is as follows:  $l = 0$  (full);  $l = 1$  (long dashes);  $l = 2$  (medium dashes);  $l = 3$  (medium dash and a dot);  $l = 4$  (medium dash and two dots);  $l = 5$  (medium dash and three dots);  $l = 6$  (medium dash and four dots).



**Table 2.** Values of the coupling constant  $\eta_0 = U_0 2m/\mu_0^2$  at which bound states of zero energy appear in the case of the exponential potential.  $l$  and  $n_r$  are the angular and the radial quantum numbers.

| <i>l</i> | <i>n<sub>r</sub></i> |            |            |            |            |            |            |
|----------|----------------------|------------|------------|------------|------------|------------|------------|
|          | 1                    | 2          | 3          | 4          | 5          | 6          | 7          |
| 1        | 1.445 7964           | 7.617 8155 | 18.721 751 | 34.760 071 | 55.733 075 | 81.640 838 | 112.483 38 |
| 1        | 7.049 0612           | 16.921 12  | 31.525 95  | 50.9476    | 75.226 12  | 104.384    | 138.433    |
| 2        | 16.312 928           | 29.879 667 | 48.076 66  | 71.002 11  | 98.7133    | 131.246    | 168.62     |
| 3        | 29.258 322           | 46.5182    | 68.3458    | 94.837     | 126.05     | 162.0      | 203        |
| 4        | 45.892 42            | 66.845 20  | 92.323     | 122.41     | 157.1      | 196        | 238        |
| 5        | 66.218 07            | 90.8638    | 120.00     | 153.7      | 191        | 233        | 276        |
| 6        | 90.2365              | 118.575    | 151.38     | 188.7      | 227        | 273        | 314        |

One may note that if *a*, *b*, *c* and *d* are four vertically or horizontally consecutive values then they are approximately related by  $a - 3b + 3c - d = 0$  and the accuracy increases with increasing quantum numbers  $n_r$  or  $l$ . This relation, therefore, is quite useful if one wants to know the values of  $\eta_0$  outside table 2. The accuracy of the relation is really amazing; for instance, for  $n_r = 7$  and  $l = 0$  the exact value given in table 2 is  $\eta_0 = 112.483\ 38$ , whereas that calculated using the above relation is  $\eta_0 = 112.483\ 36$ , so that the error is two parts in  $10^8$ . The rest of the spectrum is shown in figure 3. Figures 4(a)–(c) show the scattering cross-section  $\sigma_l(k)$  as a function of  $k/\mu_0$  for three different values of the coupling constant  $\eta_0 = U_0 2m/\mu_0^2$ . They are calculated according to (60) with  $n_{max}$  ranging from 10 to 25.

**Acknowledgments**

The author wishes to thank M Bruckheimer, J Besprosvany, Y Eisenberg, N Freed, S A Gurvitz, D Kazhdan, M Marinov, V Nabutovsky and J Pawelczyk for valuable discussions and suggestions and M Kugler for bringing the work of A Martin to the author’s attention. Part of this work was done during the author’s stay at the Institute for High Energy Physics of the ETH Zurich. The author is grateful to M Pohl and H Hofer for their hospitality. The author acknowledges support from the E P Wigner Stiftung, Berlin.

**Appendix**

The first few  $\varphi_n$  functions have a relatively simple structure. For  $l = 0$  and  $\nu = 0$  we have

$$\varphi_1(y, 0) = \frac{y}{1+y} \tag{A.1}$$

$$\varphi_2(y, 0) = \frac{y}{2+y} - \ln\left(2 \frac{1+y}{2+y}\right) \tag{A.2}$$

$$\varphi_3(y, 0) = \frac{y}{3+y} - \ln\left(\frac{3}{2} \frac{2+y}{3+y}\right) - \frac{1}{2} \ln\left(3 \frac{1+y}{3+y}\right) + \frac{1}{3+y} \ln\left(2 \frac{1+y}{2+y}\right). \tag{A.3}$$

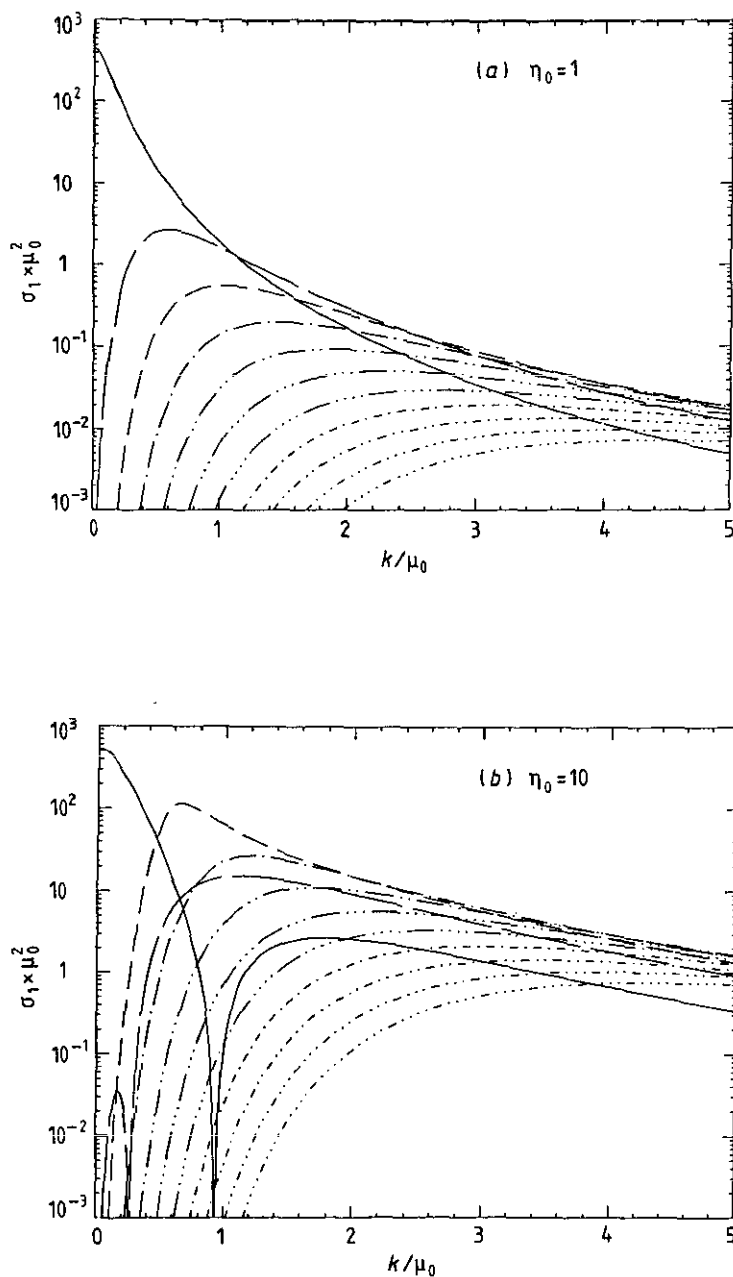


**Figure 4.** (a) Scattering cross-sections for the exponential potential for the case of a small coupling constant  $\eta_0 = U_0 2m / \mu_0^2 = 1$ . The assignment of the angular momentum quantum number  $l$  to different lines is as follows:  $l=0$  (full);  $l=1$  (long dashes);  $l=2$  (medium dashes);  $l=3$  (medium dash and a dot);  $l=4$  (medium dash and two dots);  $l=5$  (medium dash and three dots);  $l=6$  (medium dash and four dots);  $l=7$  (short dash and a dot);  $l=8$  (short dash and two dots);  $l=9$  (short dash and three dots);  $l=10$  (short dash and four dots). (b) The same as in (a) but for a larger coupling constant  $\eta_0 = 10$ . (c) The same as in (a) but for a still larger coupling constant  $\eta_0 = 30$ .

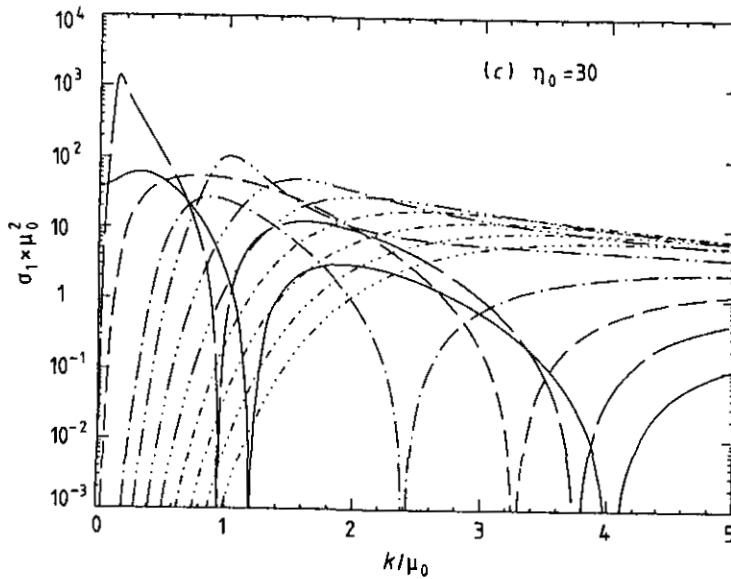


Figure 4. (continued)

For  $l=0$  we have

$$\varphi_1(y, \nu) = \frac{1}{\nu} \ln \left( \frac{(1+\nu)(1+y)}{1+\nu+y} \right) \quad (\text{A.4})$$

$$\frac{1}{n!(1+\nu/2)_n} \left( \frac{y}{n+\nu/2+y} \right)^n < \varphi_n(y, \nu) < \frac{e^{n+\nu}}{n!(1+\nu)_n} \left( \frac{y}{n+\nu+y} \right)^n \quad (\text{A.5})$$

and in particular

$$\frac{1}{n!(1+\nu/2)_n} < \varphi_n(\infty, \nu) < \frac{e^{n+\nu}}{n!(1+\nu)_n}. \quad (\text{A.6})$$

For  $\nu=0$  we have

$$\varphi_1(y, 0) = \frac{1}{2l+1} \left( \frac{y}{1+y} \right)^{2l+1} \quad (\text{A.7})$$

$$\varphi_2(y, 0) = \frac{1}{2l+1} \sum_{m=2l+2}^{\infty} \frac{1}{m} \left( -\frac{y}{2+y} \right)^m. \quad (\text{A.8})$$

## References

- [1] Martin A 1959 *Nuovo Cimento* **14** 403; 1960 *Nuovo Cimento* **15** 99; 1961 *Nuovo Cimento* **19** 1257
- [2] Martin A 1965 *Lectures on High Energy Physics* ed B Jaksic (New York: Gordon and Breach)
- [3] Poliatzky N A particle model: solution of the nonlinear Schrödinger equation in 3-D *Preprint WIS-91/81/OCT-PH*
- [4] Yukawa H 1935 *Proc. Phys. Math. Soc. Japan* **17** 48
- [5] Hulthén L and Laurikainen K V 1951 *Rev. Mod. Phys.* **23** 1
- [6] Bethe H A and Bacher R 1936 *Rev. Mod. Phys.* **8** 82

The normalized s-wave functions were derived in Roychoudhury R K 1980 *J. Phys. A: Math. Gen.* **13** L137